

Quasifragmentation functions in the massive Schwinger model

Sebastian Griener^{1,2,*} and Ismail Zahed^{1,†}

¹*Center for Nuclear Theory, Department of Physics and Astronomy,
Stony Brook University, Stony Brook, New York 11794-3800, USA*

²*Co-design Center for Quantum Advantage (C2QA),
Stony Brook University, Stony Brook, New York 11794-3800, USA*

(Dated: December 30, 2024)

We introduce the concept of the quark quasifragmentation function (qFF) using an equal-time and spatially boosted form of the Collins-Soper fragmentation function where the out-meson fragment is replaced by the current asymptotic condition. We derive the qFF for a fermion in two-dimensional quantum electrodynamics (QED2) using the Kogut-Susskind Hamiltonian after a mapping onto spin qubits in a spatial lattice with open boundary conditions. This form is suitable for quantum computations. We compute the qFF by exact diagonalization of the spin Hamiltonian. The results are compared to the qFF following from the Drell-Levy-Yan result for QED2, both at strong and weak coupling, and to two-dimensional quantum chromodynamics in the lowest Fock approximation.

I. INTRODUCTION

Parton distribution and fragmentation functions are central for the analyses of most high energy data [1, 2]. On the light front, hadrons are composed of frozen partons thanks to time dilatation and asymptotic freedom [3–5]. As a result, a hard process in quantum chromodynamics (QCD) can be split into a perturbatively calculable hard block times non-perturbative matrix elements like parton distribution functions (PDFs) and fragmentation functions (FFs).

The PDFs are valued on the light front and inherently non-perturbative, which makes them inaccessible to standard Euclidean lattice formulations, with the exception of the few lowest moments. This shortcoming is circumvented through the use of quasi-distributions [6], and their variants [7, 8]. These proposals have now been pursued by a number of QCD lattice collaborations [9–14]. We have recently shown how these concepts can be extended to quantum computation [15].

The concept of quark fragmentation, originates with the original work by Field and Feynman, who put forth the quark jet model to describe meson production in semi-inclusive processes [16]. The model is essentially an independent parton cascade model, where a hard parton depletes its longitudinal momentum by emitting successive mesons through a chain process. This idea finds a natural realization

in the string breaking at the origin of the Lund model [17]. Jet fragmentation and hadronization are vigorously pursued at current collider facilities both at the Relativistic Heavy Ion Collider and Large Hadron Collider. They be sought at the future Electron-Ion Collider to extract the partonic structure of matter, the gluon helicity in nucleons and the mechanism behind the production of diffractive dijets [18, 19].

A first principle formulation of the FFs on the light front was suggested by Collins and Soper (CS) [20]. They are fully gauge invariant but inherently non-perturbative. Remarkably, the CS FFs are still not accessible to first principle QCD lattice simulations, due to their inherent light front structure, for a review see [21]. A number of phenomenological and nonperturbative constructions have exploited crossing and analyticity symmetries, to approximate the FFs from the PDFs [22–24], as initially suggested by Drell-Levy-Yan (DLY) [25, 26].

This work is a follow up on our original work for the quasi-PDF (qPDF) using exact diagonalization of the spin Hamiltonian [15]. We will show that a first principle and non-perturbative analysis of the CS light front FFs can be obtained through suitably boosted quasi-FFs (qFFs) defined at spatial separation, where the out-going meson fragment is replaced by the current asymptotically. qFFs are readily implemented on a quantum computer using massive two-dimensional QED (QED2), the Kogut-Susskind Hamiltonian [27] on a spatial lattice with open boundary conditions. The fermion fields are eliminated by a standard Jordan-Wigner transformation [28]. Note that partonic physics on quantum

* sebastian.griener@stonybrook.edu

† ismail.zahed@stonybrook.edu

computers was also recently studied in [29–36].

This paper contains a number of new results: 1) an equal-time formulation of the FF for increasing boosts or qFF, that asymptotes the CS FF in the light-like limit; 2) explicit derivation of the DLY relation for 2D gauge theories in the light-like limit; 3) a qubit form of the qFF in QED2 for increasing boosts; 4) a numerical evaluation of the spatial correlator for the qFF in QED2 for increasing time and boosts and its comparison to the luminal CS FF. These new theoretical steps and checks are essential in assessing the FFs in a gauge theory prior to their implementation on quantum hardware.

The outline of the paper is as follows: in section II, we briefly outline the essentials of massive QED2 for this work. We introduce the concept of the quark qFF by recasting the CS light-front FF into a spatial correlator with properly boosted out-meson states. In section III, we show how the approximate DLY relation can be used to extract the qFFs from the qPDFs for QED2. In section IV, we proceed to discretize the qFF in QED2 using the Kogut-Susskind Hamiltonian on a spatial lattice with open boundary conditions. The fermion fields are eliminated with the help of a Jordan-Wigner transformation, and the ensuing qFF is shown to asymptote the CS FF for increasing boosts. Note that this formulation of the qFF can be used to perform quantum simulations on quantum hardware. Our conclusions are in section V. In the appendixes, we review a numerical algorithm for QED2 and discuss the DLY result for QCD2.

II. MASSIVE QED2

Two-dimensional QED (QED2) also known as the Schwinger model [37], exhibits a variety of non-perturbative phenomena familiar from 4-dimensional gauge theories. The extensive interest in QED2 stems from the fact that it bears much in common with two-dimensional QCD, with Coulomb law confining in two dimensions. As a result, the QED2 spectrum involves only chargeless ex-

citations. Remarkably, the vacuum state is characterized by a non-trivial chiral condensate and topologically active tunneling configurations. The massive Schwinger model is not exactly solvable and has recently received a lot of interest as a playground for quantum computations on classical and quantum hardware, see for example [38–50] and references therein. Moreover, entanglement in Schwinger pair production was investigated in [51–55].

QED2 with massive fermions is described by [37, 56]

$$S = \int d^2x \left(\frac{1}{4} F_{\mu\nu}^2 + \frac{\theta \tilde{F}}{2\pi} + \bar{\psi}(i\mathcal{D} - m)\psi \right) \quad (1)$$

with $\mathcal{D} = \not{\partial} - ig\mathcal{A}$. The bare fermion mass is m and the coupling g has mass dimension. At weak coupling with $m/g > 1$, the spectrum is composed of heavy mesons, with doubly degenerate C-even and C-odd vacua at $\theta = \pi$. At strong coupling with $m/g < 1$, the spectrum is composed of light mesons and baryons with a C-even vacuum independent of θ . Moreover, as we recently discussed in [57], in the strong coupling limit the squared rest mass may be expressed as

$$m_\eta^2 = m_S^2 + m_\pi^2 = \frac{g^2}{\pi} - \frac{m\langle\bar{\psi}\psi\rangle_0}{f_\eta^2} \quad (2)$$

with the anomalous contribution to the squared mass $m_S^2 = g^2/\pi$ and the η decay constant $f_\eta = 1/\sqrt{4\pi}$. The vacuum chiral condensate is finite in the chiral limit with $\langle\bar{\psi}\psi\rangle_0 = -\frac{e^{\gamma_E}}{2\pi} m_S$ [58, 59]. At weak coupling, the squared mass is expected to asymptote $(2m)^2$.

A. Quark FF

On the light front, a gauge-invariant definition of the QCD quark fragmentation $Q \rightarrow Q+H$ was given by Collins and Soper in [20]. When reduced to QED2 it reads

$$d_q^\eta(z, 1) = \frac{1}{z} \int \frac{dz^-}{4\pi} e^{-iz^- P^+ z^-} \text{Tr} \left(\gamma^+ \gamma^5 \langle 0 | \psi(0^-) [0^-, \infty^-]^\dagger a_{\text{out}}^\dagger(P^+) a_{\text{out}}(P^+) [\infty^-, z^-] \bar{\psi}(z^-) | 0 \rangle \right), \quad (3)$$

with a quark of longitudinal momentum $k^+ = P^+/z$ fragmenting into an on-shell $H = \eta'$ with longitudi-

nal momentum $zk^+ = P^+$. The out- η mode anni-

hilation operator is a_{out} . The holonomy along the light cone

$$[x^-, y^-] = \mathbf{P} \left(\exp \left(-ig \int_{x^-}^{y^-} dz^- A^+(z^-) \right) \right) \quad (4)$$

can be omitted in the light-cone gauge. Eq. (3) can be regarded as the number of η s of momentum P^+ in a fast moving quark (dressed by a gauge holonomy) of momentum P^+/z . Our conventions for the gamma matrices are $\gamma^0 = \sigma^3$ and $\gamma^1 = i\sigma^2$, with $\gamma^+ = \gamma^0 + \gamma^1$ and $\bar{\psi}\gamma^+\gamma^5\psi = \bar{\psi}\gamma^+\psi$.

Using the ‘‘good’’ component of the fermionic field in light front quantization, and setting the gauge links to 1, (3) can be recast as

$$d_\eta^q(z) = \frac{dP^+}{dz} \frac{\langle k^+ | a_{\text{out}}^\dagger(P^+) a_{\text{out}}(P^+) | k^+ \rangle}{\langle k^+ | k^+ \rangle} \quad (5)$$

which is the light cone momentum distribution of the meson η in the quark q (dressed by the holonomy).

It satisfies the momentum sum rule

$$\int_0^1 dz z d_\eta^q(z) = 1 \quad (6)$$

provided that the quark state is an eigenstate of the **mesonic** momentum operator,

$$\left(\mathbb{P} = \int dP^+ P^+ a_{\text{out}}^\dagger(P^+) a_{\text{out}}(P^+) \right) |k^+\rangle = k^+ |k^+\rangle \quad (7)$$

In the absence of a conserved charge in massive QED2,

$$\int_0^1 dz d_\eta^q(z) = \frac{\langle k^+ | \mathbb{Q} = \int dP^+ a_{\text{out}}^\dagger(P^+) a_{\text{out}}(P^+) | k^+ \rangle}{\langle k^+ | k^+ \rangle} \quad (8)$$

is not normalized to 1, as the number of out-going mesons is not fixed. The generalization to multiflavor QED2 would lead to conserved flavor charges.

B. Quark qFF

With this in mind, we introduce the qFF for QED2

$$d_q^\eta(z, v) = \frac{1}{z} \int \frac{dZ}{4\pi} e^{-i\frac{1}{z}P(v)Z} \text{Tr} \left(\gamma^+ \gamma^5 \langle 0 | \psi(0) [0, \infty]^\dagger a_{\text{out}}^\dagger(P(v)) a_{\text{out}}(P(v)) [\infty, Z] \bar{\psi}(Z) | 0 \rangle \right) \quad (9)$$

or the equivalent but spatially symmetric form

$$d_q^\eta(z, v) = \frac{1}{z} \int \frac{dZ}{4\pi} e^{-i(\frac{z}{z}-1)P(v)Z} \text{Tr} \left(\gamma^+ \gamma^5 \langle 0 | \psi(-Z) [-Z, \infty]^\dagger a_{\text{out}}^\dagger(P(v)) a_{\text{out}}(P(v)) [\infty, Z] \bar{\psi}(Z) | 0 \rangle \right) \quad (10)$$

where $P(v) = \gamma(v)m_\eta v$ is the momentum fraction carried by the emitted η from a mother quark jet with momentum $P(v)/z$. Eq. (9) is seen to reduce to the light front FF (3) in the luminal limit $v \rightarrow 1$. Here the holonomies are running along the spatial direction. In two dimensions, both gauge degrees of freedom $A^{0,1}$ can be eliminated by our gauge choice $A^0 = 0$, and using Gauss law which will be carried out below.

The out- η field canonical decomposition in normal modes is given by

$$\eta_{\text{out}}(x) = \int \frac{dk}{4\pi k^0} (a_{\text{out}}(k) e^{-ik \cdot x} + a_{\text{out}}^\dagger(k) e^{+ik \cdot x}) \quad (11)$$

with the on-shell energy $k^0 = E_k = \sqrt{k^2 + m_\eta^2}$. The

asymptotic current condition

$$\bar{\psi} \gamma_\mu \gamma_5 \psi(x) \rightarrow F \partial_\mu \eta_{\text{out}}(x) \quad x^0 \rightarrow +\infty \quad (12)$$

with $F = \sqrt{2}f$, defines

$$\frac{F i q_\mu}{2q^0} a_{\text{out}}^\dagger(q) = \int dx e^{-iE_q t + i q x} \bar{\psi} \gamma_\mu \gamma_5 \psi(t, x) |_{t \rightarrow +\infty} \quad (13)$$

or equivalently

$$a_{\text{out}}^\dagger(q) = \frac{-2i}{F} e^{-iE_k t} \psi^\dagger \gamma_5 \psi(t, q) |_{t \rightarrow +\infty}. \quad (14)$$

The asymptotic time limit implements the Lehmann-Symanzik-Zimmermann (LSZ) reduction on the source field. If we denote the (normal

ordered) Hamiltonian operator in temporal gauge by \mathbb{H} , then we find

$$a_{\text{out}}^\dagger(P)a_{\text{out}}(P) = \frac{4}{F^2} e^{i\mathbb{H}t} |\psi^\dagger \gamma_5 \psi(0, P(v))|^2 e^{-i\mathbb{H}t} |_{t \rightarrow +\infty}. \quad (15)$$

The symmetric qFF (10) can be recast in terms of the spatial qFF correlator

$$d_q^n(z, v) = \frac{1}{z} \int \frac{dZ}{4\pi} e^{-i(\frac{z}{2}-1)P(v)Z} \mathbb{C}(Z, v, \infty) \quad (16)$$

with

$$\mathbb{C}(Z, v, t) = \frac{4}{F^2} \text{Tr} \left(\gamma^+ \gamma^5 \langle 0 | \psi(0, -Z) [-Z, \infty]^\dagger e^{i\mathbb{H}t} e^{i\chi(v)\mathbb{K}} | \psi^\dagger \gamma_5 \psi(0, 0) \rangle^2 e^{-i\chi(v)\mathbb{K}} e^{-i\mathbb{H}t} [\infty, Z] \bar{\psi}(0, Z) | 0 \rangle \right). \quad (17)$$

In QED2 in the temporal gauge $A^0 = 0$, the Hamiltonian and boost operators associated to (1) are

$$\begin{aligned} \mathbb{H} &= \int dx \left(\frac{1}{2} E^2 + \psi^\dagger (i\alpha D_x + m\gamma^0) \psi \right), \\ \mathbb{K} &= \int dx x \left(\frac{1}{2} E^2 + \psi^\dagger (i\alpha D_x + m\gamma^0) \psi \right) \end{aligned} \quad (18)$$

and satisfy the Poincare algebra

$$[\mathbb{K}, \mathbb{H}] = i\mathbb{P}, \quad (19)$$

$$[\mathbb{K}, \mathbb{P}] = i\mathbb{H}, \quad (20)$$

with the momentum operator \mathbb{P} . The rapidity is

defined as

$$\chi(v) = \frac{1}{2} \ln \left(\frac{1+v}{1-v} \right). \quad (21)$$

Note that under the combined boost and time evolution, the equal-time fermion field is now lying on the light cone, e.g.

$$\begin{aligned} e^{-i\chi(v)\mathbb{K}} e^{-i\mathbb{H}t} \bar{\psi}(0, \pm Z) e^{i\mathbb{H}t} e^{i\chi(v)\mathbb{K}} \\ = \bar{\psi}(-\gamma(v)(t \pm vZ), \gamma(v)(vt \pm Z)) S^{-1}[v] \end{aligned} \quad (22)$$

with $S[v] = e^{\frac{1}{2}\chi(v)\gamma^5}$, for which (17) in the temporal gauge reads

$$\mathbb{C}(Z, v, t) = \frac{4}{F^2} \text{Tr} \left(\gamma^+ \gamma^5 \langle 0 | \psi(-\gamma(v)(t - vZ), \gamma(v)(-Z + vt)) | \psi^\dagger \gamma_5 \psi(0, 0) \rangle^2 \bar{\psi}(-\gamma(v)(t + vZ), \gamma(v)(vt + Z)) | 0 \rangle \right). \quad (23)$$

III. DRELL-LEVY-YAN IN 2D

Crossing symmetry and charge conjugation allow for an estimate of the CS FF in terms of the parton distribution functions using the DLY relation [25]. This observation carries to the primitive qFF with the DLY relation

$$d_{DLY}(z, v) = \frac{z^{d-3}}{de} p_\eta \left(\frac{1}{z}, v \right) \quad (24)$$

where de is a pertinent degeneracy factor which is 1 in QED2 and N_c in QCD2. For QED2, the PDF is briefly reviewed in Appendix A and the qPDF in [15]. Inserting (24) into (16) and inverting yield

the DLY spatial correlator ($\bar{z} = 1 - z$)

$$\mathbb{C}_{DLY}(Z, v, \infty) = 4P \int dz e^{i(z-\bar{z})P(v)Z} |\varphi_\eta(z, v)|^2. \quad (25)$$

The DYL relation can be readily applied to QED2 using the PDFs or qPDFs in [15]. Since the qPDFs were obtained using an expansion in Jacobi polynomials of increasing powers, the substitution $x \rightarrow 1/z$ is increasingly singular. To circumvent this, we can use the exact equation (A1) with the normalized solution $\int dx \varphi(x) = f$, to rewrite (24) as

$$d_{DLY}(z, 1) = \frac{\bar{z}^2}{z(\bar{z}\mu^2 + z^2\bar{\alpha})^2} \left(f - \int_0^1 dx \frac{\varphi(x)}{(x - 1/z)^2} \right)^2 \quad (26)$$

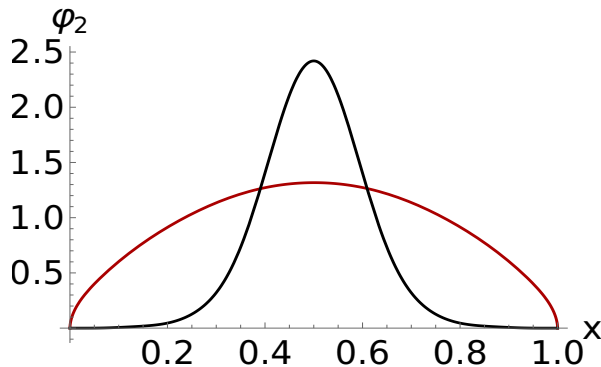


FIG. 1: Solution to (A1) for $\beta = \sqrt{3}/\pi$ (red) and $\beta = 10\sqrt{3}/\pi$ (black) using 13 Jacobi polynomials.

with $\mu^2 = M^2/m_S^2$ and $1 + \bar{\alpha} = \alpha = m^2/m_S^2$. We have dropped the principal part prescription since $0 \leq z \leq 1$ with $\varphi(x)$ vanishing at the end points. A sample of the light front wave functions solution to (A1) is shown in Fig. 1 for strong (solid red line) and weak coupling (solid black line).

A. Light masses

In the massless limit, (26) simplifies to

$$d_{DLY}(z, 1) \rightarrow \frac{1}{z} \quad (27)$$

following the substitutions $\varphi(x) \rightarrow \theta(x\bar{x})$, $f \rightarrow 1$, $\mu^2 \rightarrow 1$ and $\bar{\alpha} \rightarrow -1$. The apparent singularity in the denominator of (26) at $\bar{z} = z^2$, is canceled by the numerator. We also expect this cancellation to happen in the massive case provided that the exact wave functions are used. For small masses $m/m_S < 1$, (26) scales as $d_\eta(z \sim 0, 1) \sim 1/z$ and vanishes as $d_\eta(z \sim 1, 1) \sim \bar{z}^{2\beta}$ since

$$\left(f - \int_0^1 dx \frac{\varphi(x)}{(x - 1/z)^2} \right)_{z \rightarrow 1}^2 \approx \bar{z}^{2(\beta-1)} \left(\int_0^\infty ds \frac{s^\beta}{(1+s)^2} \right)^2 \quad (28)$$

following the variable shift $\bar{x} = s\bar{z}$ in the integral.

A useful approximation for light quark masses is to use the leading 0th Jacobi polynomial in (A6)

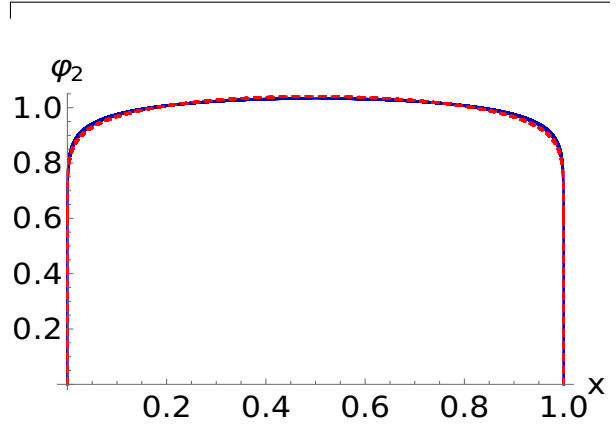


FIG. 2: Lowest state wave function in QED2 using the 0th Jacobi polynomial (solid red line) and a basis with 13 Jacobi polynomials (solid blue line).

(solid red line) which compares well with the solution obtained using 13 Jacobi polynomials (solid blue line) for the ground state as shown in Fig. 2. When inserted in the DLY result, the approximated form is

$$d_{DLY}(z, 1) \rightarrow \frac{\Gamma(2 - 2\beta)}{\Gamma(1 - 4\beta)\Gamma(1 + 2\beta)} \frac{\bar{z}^{2\beta}}{z^{1+4\beta}} \quad (29)$$

with the normalization adjusted to satisfy the momentum sum rule (6). The solution (29) also shows the expected end point behavior in the strong coupling regime, with β satisfying

$$\beta = \frac{\sqrt{3}}{\pi} \frac{m}{m_S} < \beta_c = \frac{\sqrt{3}}{\pi\sqrt{\pi}}.$$

In Fig. 3 we show the behavior of (29) for $\beta = 0$ (solid blue) and $\beta = 0.2$ (solid red) in the strong coupling regime. The fragmentation function vanishes in the forward direction $z \rightarrow 1$, and diverges as $z \rightarrow 0$. The divergence in the $m/m_S \rightarrow 0$ limit is in agreement with the exact bosonization description in QED2 [60]. In this dual limit, the FF follows from coherent emission from a classical field sourced by light-like currents using bosonization.

B. Heavy masses

In the heavy quark limit $m/m_S \gg 1$, the anomaly drops out which amounts of dropping the

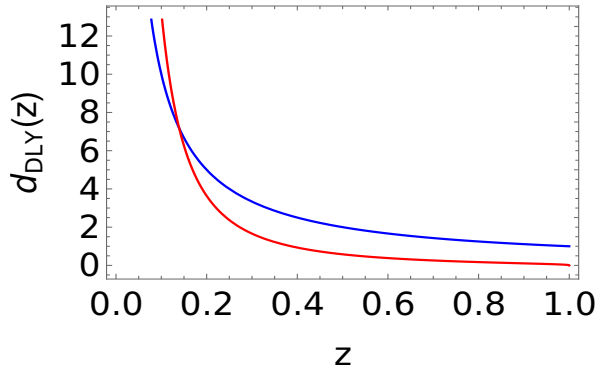


FIG. 3: DLY fragmentation function for light quarks in the strong coupling regime: $\beta = 0$ (solid blue) and $\beta = 0.2$ (solid red) as in (29).

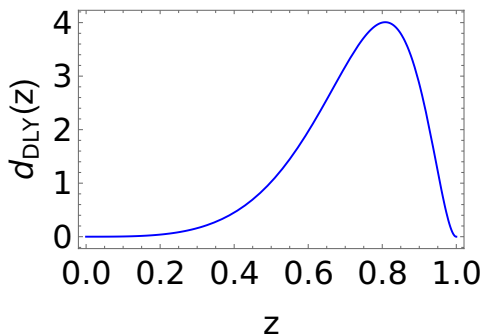


FIG. 4: DLY fragmentation function for heavy quarks in QED2 as in (30).

f -contribution in the bracket in (26). In this limit, we have $\varphi(x) \rightarrow f_H \delta(x - 1/2)$, $\mu^2 \rightarrow 4\alpha$ and $\bar{\alpha} \rightarrow \alpha$, with the result

$$d_{DLY}(z, 1) \rightarrow \frac{16f_H^2}{\alpha^2} \frac{z^3 \bar{z}^2}{(z-2)^8}. \quad (30)$$

The constant f_H is fixed by the momentum sum rule

$$\int_0^1 dz z d_{DLY}(z, 1) = \frac{2f_H^2}{105\alpha^2} \rightarrow 1. \quad (31)$$

In Fig. 4, we show the result (30) with the vanishing of the FF at both end points. For heavy fermions, the FF is peaked in the forward (jet) direction, with a strong suppression as $z \rightarrow 0$.

To address the fragmentation for heavy but finite mass in the 2-particle Fock space, a useful approximation is to map the light-front equation for the wave functions onto a standard Schrödinger equation. This is achieved by noting that (A1) follows from the light-front quantization of a two dimensional string with massive end points much like in

QCD2 [61, 62], modulo the U(1) anomaly which drops out in the heavy mass limit. With this in mind, the equal-time quantization for large masses yields [61–63]

$$-\frac{1}{m} \varphi_n''(r) + 2\pi m_S^2 |r| \varphi_n(r) = (E_n - 2m) \varphi_n(r) \quad (32)$$

with r being the relative separation between the heavy pair. The solutions are Airy functions ($r \geq 1$)

$$\varphi_n^+(r) = \text{Ai} \left((2\pi m_S^2 m)^{\frac{1}{3}} (r - (E_n - 2m)/(2\pi m_S^2)) \right) \quad (33)$$

and $\varphi_n^-(r) = (-1)^n \varphi_n^+(-r)$ for $r < 0$, with eigen-energies

$$E_n = 2m - \left(\frac{(2\pi m_S^2)^2}{m} \right)^{\frac{1}{3}} r_n \quad (34)$$

where r_n is the n th zero of the Airy function or its derivative. The relationship to the distribution amplitudes (DAs) follows by Fourier inverse

$$\varphi_n(\xi) = \int_{-\infty}^{+\infty} \frac{ds}{2\pi} e^{-is\xi} (\theta(s) \varphi_n^+(s) + \theta(-s) \varphi_n^-(s)) \quad (35)$$

after the rescaling $s = m_S r$, with the symmetric parton fraction $\xi = 2x - 1$.

IV. LATTICIZED KOGUT-SUSSKIND HAMILTONIAN

In this section, we explain how we discretize the Hamiltonian (1) on a lattice of length $L = Na$. Using staggered fermions, the discretization of the two-dimensional massive Schwinger model and gauge fixing is standard [64].

A. Details of the lattice

Using the Kogut-Susskind Hamiltonian formulation, the staggered fermions are mapped onto a spatial lattice by assigning the upper component of the bispinor to even sites and the lower component to odd sites,

$$\psi(0, z = na) = \frac{1}{\sqrt{a}} \begin{pmatrix} \psi_e(n) \\ \psi_o(n) \end{pmatrix} = \frac{1}{\sqrt{a}} \begin{pmatrix} \varphi_{n:\text{even}} \\ \varphi_{n+1:\text{odd}} \end{pmatrix} \quad (36)$$

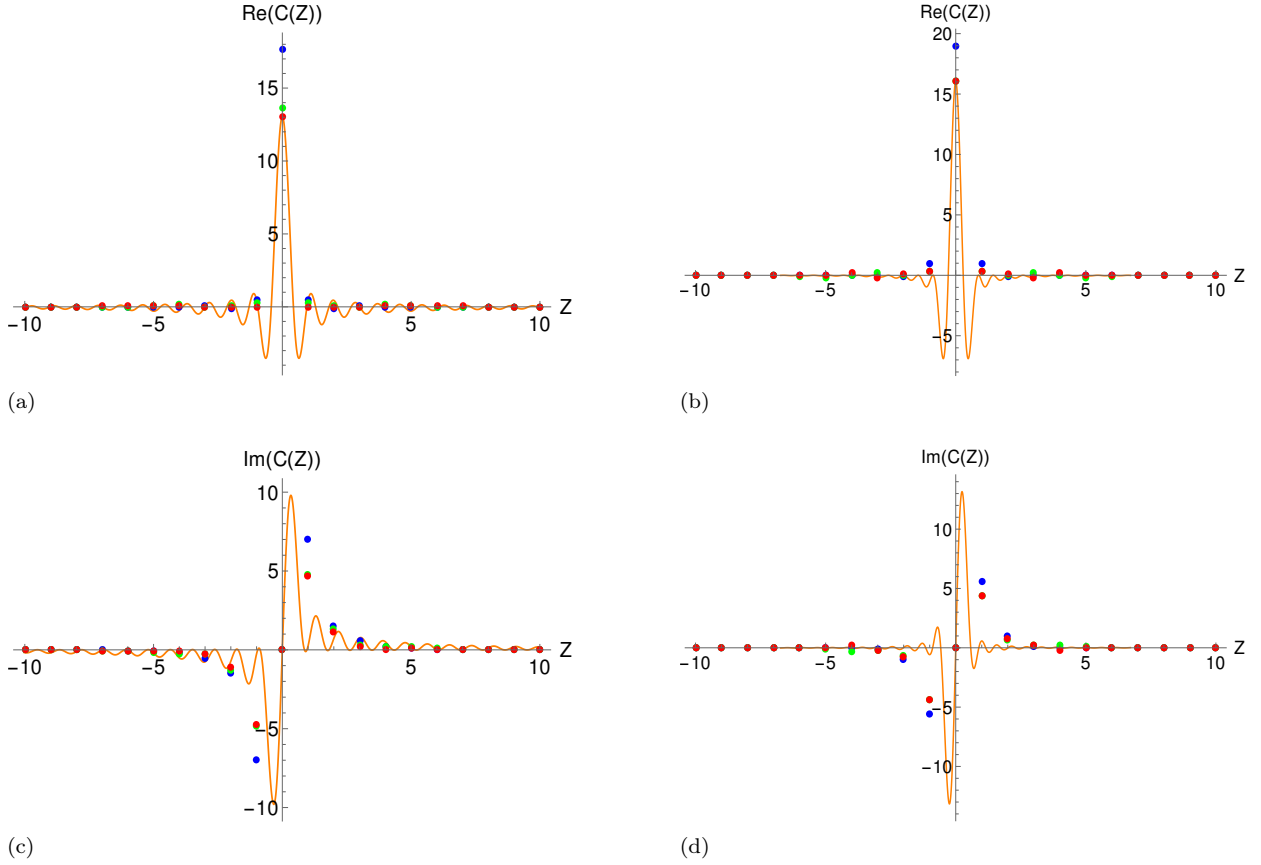


FIG. 5: $\text{Re } C(Z)$ in (a,b) and $\text{Im } C(Z)$ in (c, d) for $m/m_S = 0.177$ (left panel) and $m/m_S = 0.806$ (right panel) for a boost with $v = 0.925$ at times $t = 0.1$ (blue dots), $t = 13$ (green dots), $t = 25$ (red dots) using the improved lattice mass. The solid line (solid orange line) is the light front result with $v = 1$ in (25) using the solution to (A1) with 19 Jacobi polynomials. The orange line is rescaled to match the maximum of the real part at $Z = 0$ (for $t = 13$). For the lattice data, we fixed $N = 22$ and $g = 1$. The data is shown in units of $a = 1$.

with $0 \leq n \leq N - 1$. The chiral fermions map onto $\psi_e(n) = \varphi_n$ (even sites) and $\psi_o(n) = \varphi_n$ (odd sites), with

$$\begin{aligned}\varphi_n &= \prod_{m < n} [+iZ_m] \frac{1}{2} (X_n - iY_n), \\ \varphi_n^\dagger &= \prod_{m < n} [-iZ_m] \frac{1}{2} (X_n + iY_n).\end{aligned}\quad (37)$$

The boost operator maps onto

$$\begin{aligned}\mathbb{K} \rightarrow & \frac{1}{2} g^2 a^2 \sum_{n=0}^{N-1} n L_n^2 \\ & + \frac{1}{4} \sum_{n=0}^{N-1} n (X_n X_{n+1} + Y_n Y_{n+1}) \\ & + \frac{ma}{2} \sum_{n=0}^{N-1} (-1)^n n (1 + Z_n).\end{aligned}\quad (38)$$

Moreover, the lattice Hamiltonian reads [64]

$$\begin{aligned}\mathbb{H} \rightarrow & \frac{1}{4a} \sum_{n=1}^{N-1} (X_n X_{n+1} + Y_n Y_{n+1}) \\ & + \frac{m}{2} \sum_{n=1}^N (-1)^n Z_n + \frac{ag^2}{2} \sum_{n=1}^{N-1} L_n^2,\end{aligned}\quad (39)$$

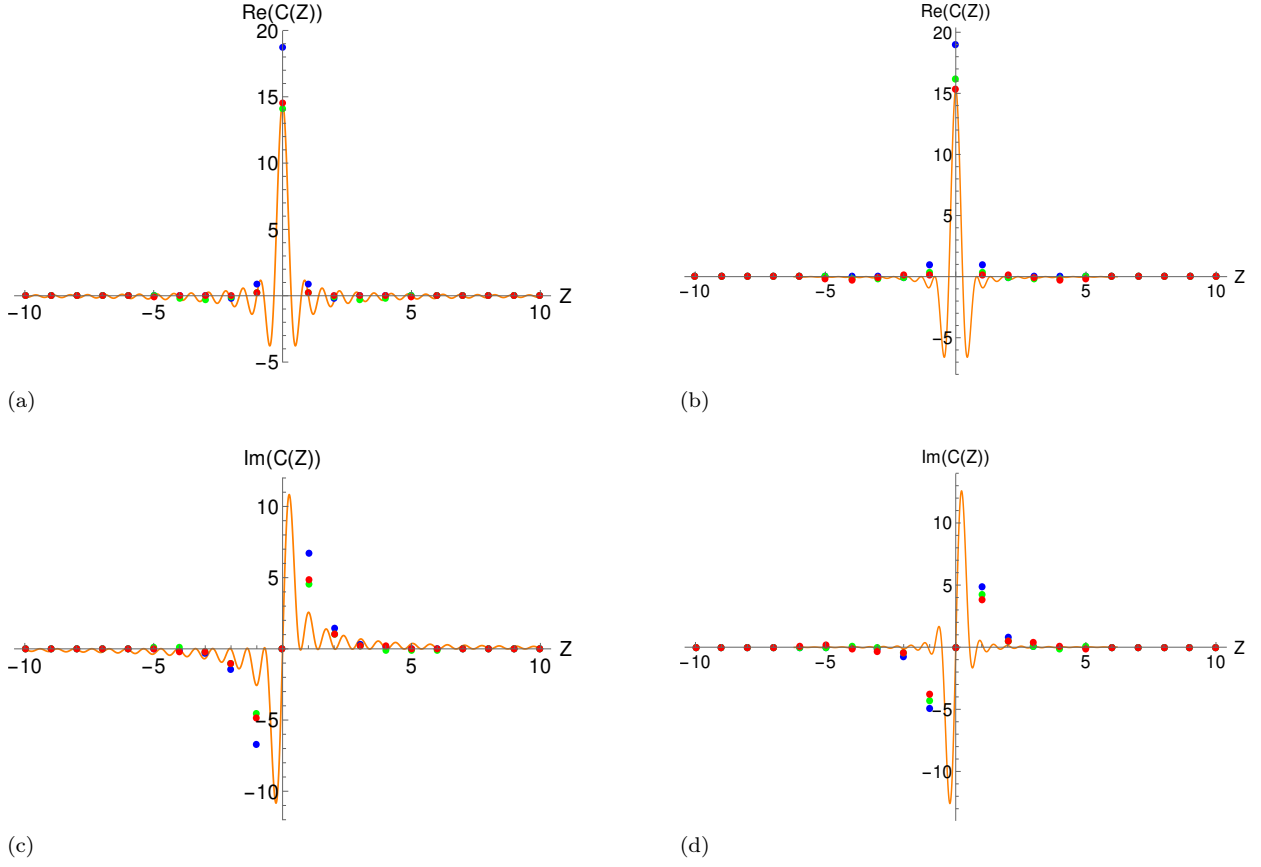


FIG. 6: $\text{Re } C(Z)$ in a,b and $\text{Im } C(Z)$ in c, d for $m/m_S = 0.177$ (left panel) and $m/m_S = 0.806$ (right panel) for a boost with $v = 0.925$ at times $t = 0.1$ (blue dots), $t = 13$ (green dots), $t = 25$ (red dots) using the *naïve* lattice mass. The solid line (solid orange line) is the light front result with $v = 1$ in (25) using the solution to (A1) with 19 Jacobi polynomials. The orange line is rescaled to match the maximum of the real part at $Z = 0$ (for $t = 13$). For the lattice data, we fixed $N = 22$ and $g = 1$. The data is shown in units of $a = 1$.

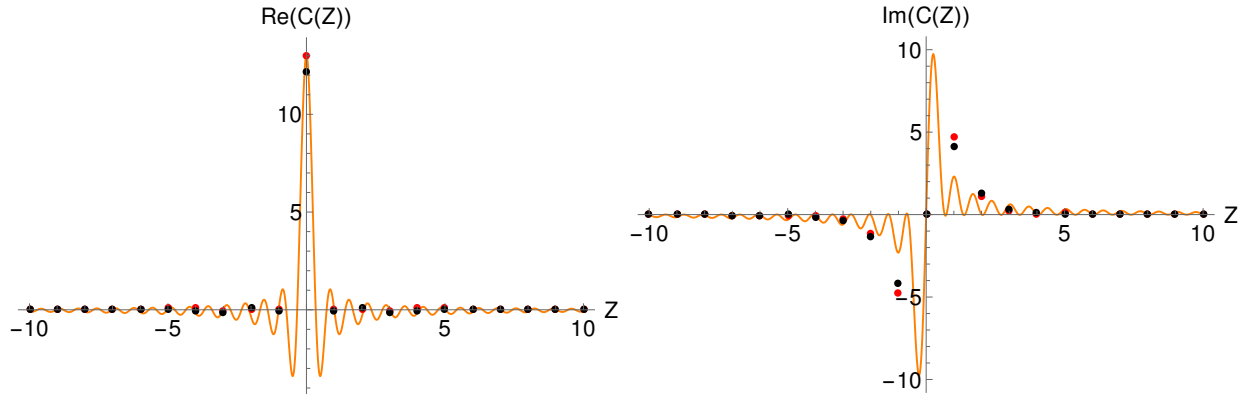


FIG. 7: Comparison of the spatial qFF for the boosted (42) (black) and unboosted form (43) (red). We fixed $N = 22$, $t = 25$, $g = 1$, $v = 0.925$ and $m/m_S = 0.177$ using the improved lattice mass, all in units of $a = 1$.

where L_n is the local electric field operator

$$L_n = \sum_{j=1}^n \frac{Z_j + (-1)^j}{2}. \quad (40)$$

$$\mathbb{C}(n, v, t) = \frac{4}{aF^2} \sum_{i,j=e,o} \langle 0 | \psi_i(-n) e^{i\mathbb{H}t} e^{i\chi(v)\mathbb{K}} |\psi^\dagger \gamma_5 \psi(0, 0)|^2 e^{-i\chi(v)\mathbb{K}} e^{-i\mathbb{H}t} \psi_j^\dagger(n) |0\rangle. \quad (42)$$

or equivalently

$$\mathbb{C}(n, v, t) = \frac{4}{aF^2} \sum_{i,j=e,o} \langle 0 | \psi_i(-n) e^{i\mathbb{H}t} |\psi^\dagger \gamma_5 \psi(0, P(v))|^2 e^{-i\mathbb{H}t} \psi_j^\dagger(n) |0\rangle. \quad (43)$$

with the fully boosted source

$$|\psi^\dagger \gamma_5 \psi(0, P(v))|^2 = \frac{1}{a^2} \left| \sum_n e^{iP(v)na} (\sigma_n^+ \sigma_{n+1}^- - \sigma_{n+1}^+ \sigma_n^-) \right|^2. \quad (44)$$

To proceed, the ground state is obtained as the lowest state of the spin qubit Hamiltonian following from an exact diagonalization of the Hamiltonian (39). Eq. (42) is then evaluated by first applying the double unitary evolutions, and then measuring (41) at large times t for increasing rapidities χ . In Fig. 5, we show the numerical results for the real (Re) and imaginary (Im) parts of the spatial correlator qFF (42) in the strong coupling regime with $m/m_S = 0.177$ (left panel) and the weak coupling regime with $m/m_S = 0.806$ (right panel) using the improved lattice mass [65] as discussed in [15]. The results using the *naïve* lattice mass are shown in Fig. 6.

The results for the correlators are at time $t = 0.1$ (blue dots), $t = 13$ (green dots) and $t = 25$ (red dots) for a fixed boost velocity $v = 0.925$ and $N = 22, g = a = 1$. The solid curve (solid orange line) is the light-front result with $v = 1$, for the spatial correlator (25) following from the solution to (A1), in the lowest Fock approximation. Since

B. Lattice qFF from Exact Diagonalization

The discretization of the qFF in QED2 follows the same line of arguments as the one of the qPDFs in [15]. The only new element is

$$|\psi^\dagger \gamma_5 \psi(0, 0)|^2 = \frac{1}{a^2} \left| \sum_n (\sigma_n^+ \sigma_{n+1}^- - \sigma_{n+1}^+ \sigma_n^-) \right|^2, \quad (41)$$

where $\sigma_n^\pm = \frac{1}{2}(X_n \pm iY_n)$. With this in mind, the discretized form of the symmetric spatial qFF (17) reads

the DLY relation is an approximation to the FF, the comparison is only qualitative. Note that the spatial correlator (42) is evaluated for large times $t \gg m_S \sim g/\sqrt{\pi}$. Finally, we have checked that our numerical results converge sufficiently fast above this time scale which is explicitly demonstrated in appendix C.

In Fig. 7, we compare the numerical results stemming from the boosted form (42) and the unboosted form (43). The differences stem from the numerical discretization of the boost operator on this coarse lattice. In particular, we discussed the numerical errors arising from the discretized version of the boost in our previous publication [15].

V. CONCLUSIONS

We have shown that the CS FFs can be obtained through equal-time and properly boosted qFFs defined at spatial separation, with the out-going meson fragment sourced by a pertinent current condition at large times. This construction was explicitly implemented in massive QED2, where the FF follows from a combination of boosts and large time evolution.

We have used the DLY result for the FF in QED2,

to derive explicit forms for the FFs and to analyze their behavior in the strong and weak coupling regimes. In the 2-Fock space approximation, the QED2 results readily extend to QCD2 with minor changes.

Using the Kogut-Susskind Hamiltonian on a spatial lattice with open boundary conditions, we discretized massive QED2 using a spin formulation suitable for quantum computations. The qFF is reduced to a Fourier transform of a spacial correlator at fixed boost and large time, on a spatial lattice with open boundary. We have shown that for increasing boosts and large times the results from exact diagonalization for the qFF are in fair agreement with the corresponding DLY correlator in the light-like limit.

The spin formulation we used, readily maps onto qubits for a full quantum computation. More importantly, our suggested qFF can be evaluated in full QCD using the gauged fixed Kogut-Susskind lattice Hamiltonian formulation with continuous time [27]. We plan to report on some of these issues next.

ACKNOWLEDGMENTS

This work is supported by the Office of Science, U.S. Department of Energy under Contract No. DE-FG-88ER40388. The work of S.G. is supported by the U.S. Department of Energy, Office of Science, National Quantum Information Science Research Centers, Co-design Center for Quantum Advantage (C2QA) under Contract No. DE-SC0012704. S.G. is also in part supported by a Feodor Lynen Research fellowship of the Alexander von Humboldt foundation. This research is also supported in part within the framework of the Quark-Gluon Tomography (QGT) Topical Collaboration, under Contract No. DE-SC0023646.

Appendix A: η DA and PDF

In the 2-particle Fock-space approximation, the light front wave functions DAs $\varphi_n(x)$ for QED2 follow from [66]

$$\mu^2 \varphi(x) = \int_0^1 dy \varphi(y) + \frac{\alpha}{x\bar{x}} \varphi(x) - \text{PP} \int_0^1 dy \frac{\varphi(y) - \varphi(x)}{(x-y)^2} \quad (\text{A1})$$

with xP being the momentum fraction of the partons. Here PP is short for the principal part, and the masses are rescaled

$$\mu^2 = M^2/m_S^2, \quad \alpha = m^2/m_S^2.$$

The longitudinal kinetic contribution (second term on the RHS) is singular at $x = \pm 1$, forcing the light front wave function to vanish at the edges $\varphi_n(\pm 1) = 0$.

In the massless limit with $m \rightarrow 0$, the spectrum is that of a single massive boson

$$\varphi_\eta(x) = \varphi_0(x) \rightarrow \theta(x\bar{x}), \quad M_0^2 \rightarrow m_S^2. \quad (\text{A2})$$

For small m , the lowest solution vanishes at the end points as powers of m , $\varphi_n(x) \sim (x\bar{x})^\beta$ with β fixed by [67]

$$\frac{m^2}{m_S^2} = 1 - \pi\beta \cotan(\pi\beta). \quad (\text{A3})$$

In the massive limit with $m \gg m_S$, the solution is peaked around $x = \frac{1}{2}$, with $M \approx 2m$. The lowest

state parton distribution function is of the form

$$q_\eta(x) = |\varphi_\eta(x)|^2. \quad (\text{A4})$$

The general solution to (A1) can be obtained through numerical diagonalization, using the basis expansion [68]

$$\varphi(x) = \sum_n \bar{c}_n \bar{f}_n(x) \quad (\text{A5})$$

with Jacobi polynomials

$$\bar{f}_n(x) = \bar{C}_n (x\bar{x})^\beta P_n^{(2\beta, 2\beta)}(x - \bar{x}) \quad (\text{A6})$$

normalized through

$$\bar{C}_n = \left(n!(1+2n+4\beta) \frac{\Gamma(1+n+4\beta)}{\Gamma^2(1+n+2\beta)} \right)^{\frac{1}{2}}.$$

The matrix form of (A1) is

$$(\bar{\mathbb{A}}_{mn} + \bar{\mathbb{B}}_{mn} + \bar{\mathbb{C}}_{mn}) \bar{c}_n = \mu^2 \bar{c}_m \quad (\text{A7})$$

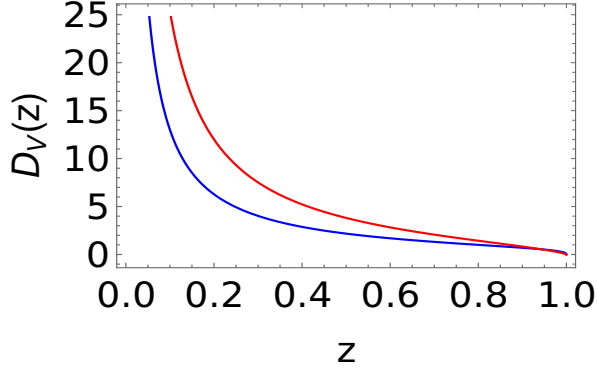


FIG. 8: Fragmentation function for light quarks from QCD2, following from the leading planar contribution in (B4) from [69].

with the matrix entries

$$\begin{aligned}\bar{\mathbb{A}}_{mn} &= \int_0^1 dx dy \bar{f}_m(x) \bar{f}_n(y) \\ \bar{\mathbb{B}}_{mn} &= \alpha \int_0^1 dx \frac{\bar{f}_m(x) \bar{f}_n(x)}{x\bar{x}} \\ \bar{\mathbb{C}}_{mn} &= -\text{PP} \int_0^1 dx dy \frac{\bar{f}_m(x)(\bar{f}_n(y) - \bar{f}_n(x))}{(x-y)^2}.\end{aligned}\tag{A8}$$

The procedure for the diagonalization was recently detailed in [15] (and references therein).

Appendix B: DLY in QCD2

Given the similarity between (A1) in the 2-Fock space approximation, and the 't Hooft equation for QCD2 in the large N_c limit on the light front (suppressed vacuum contributions), we conclude that the DLY fragmentation of a quark $Q_f \rightarrow Q_f + n$ in

$$\frac{d \ln \sigma_n}{dz} = (d_V^n(z) + d_{\bar{V}}^n(z)) = \frac{C_n}{z} \left(\left| \frac{1}{z} \int_z^1 dy \int_0^1 dx \frac{\varphi_n(x)}{(x-y/z)^2} \right|^2 + \left| \frac{1}{z} \int_0^{\bar{z}} dy \int_0^1 dx \frac{\varphi_n(x)}{(x-(y-\bar{z})/z)^2} \right|^2 \right).\tag{B4}$$

with d_V^n and $d_{\bar{V}}^n$ identified with the first and second

QCD2 gives

$$d_{DLY}^n(z, 1) \rightarrow \frac{1}{N_c} \frac{\bar{z}^2}{z(\bar{z}\mu^2 + z^2\bar{\alpha})^2} \left(\int_0^1 dx \frac{\varphi_n(x)}{(x-1/z)^2} \right)^2\tag{B1}$$

and $m_S^2 \rightarrow \lambda/2\pi$ with fixed 't Hooft coupling $\lambda = g^2 N_c$. Recall that in QCD2 there is no $U(1)$ anomaly, so the f -contribution drops out from the squared bracket in (B1). This result is in agreement with the one recently derived in [70], using the $1/N_c$ counting in light front perturbation theory.

In the massless limit, the 't Hooft equation admits a massless mode with $\varphi_0(x) = \theta(x\bar{x})$ and $\mu = 0$ (would-be Goldstone mode), for which (B1) simplifies

$$d_{DLY}^0(z, 1) \rightarrow \frac{1}{N_c z}\tag{B2}$$

and normalizes to $1/N_c$ for each quark color. In the massive but strong coupling case, the massless mode turns massive with $\varphi_0(x) \approx (x\bar{x})^\beta$ and $\mu^2 \approx m/m_S$. Eq. (B1) is apparently singular, but reverting to the original DLY form

$$d_{DLY}^n(z, 1) \rightarrow \frac{1}{N_c z} \left| \varphi_n \left(\frac{1}{z}, 1 \right) \right|^2\tag{B3}$$

yields a similar result to QED2 under the substitution $\varphi_0(x) \approx (x\bar{x})^\beta$ for light quark masses. In the heavy mass limit, the DLY fragmentation function for QCD2 is in total agreement with QED2, once the momentum sum rule is enforced.

The result (B1) is of order $1/N_c$ for each quark color and flavor and sums up to N_c^0 at variance with expectations from duality where it should reduce to the famed R-ratio of order N_c . Indeed, in [69] it was argued that the DLY relation in QCD2 does not yield the expected R-ratio scaling in the 't Hooft limit. In this limit, the annihilation $e^+e^- \rightarrow X$ in terms of planar diagrams proceeds solely through meson decays. For a meson decay to a pair of mesons $V \rightarrow V + n$, the result is [69]

contributions, respectively. It is of order N_c^0 as well

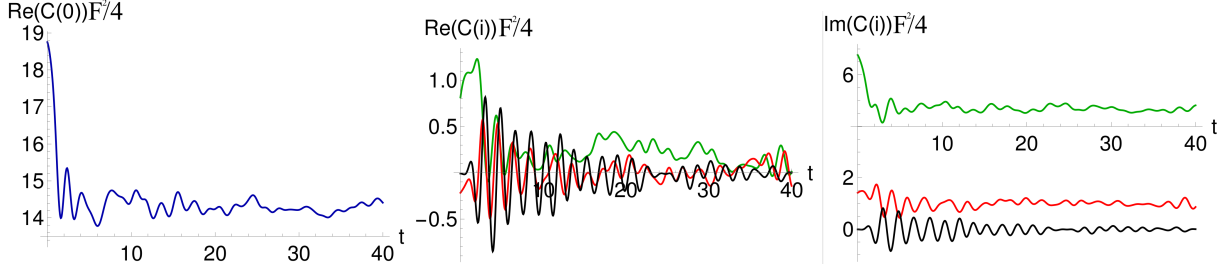


FIG. 9: *Left:* $\text{Re}(C(0))$, *Middle:* $\text{Re}(C(1))$ (green), $\text{Re}(C(2))$ (red), $\text{Re}(C(3))$ (black), *Right:* $\text{Im}(C(1))$ (green), $\text{Im}(C(2))$ (red), $\text{Im}(C(3))$ (black), as a function of time. We fixed $N=18$, $g = 1$ and $m/m_S = 0.806$ using the improved lattice mass; all plots are in units of $a = 1$.

for each meson state lying on the radial Regge trajectory (see below). Here C_n is fixed by the momentum sum rule

$$\int_0^1 dz \frac{d\ln\sigma_n}{d\ln z} = 1. \quad (\text{B5})$$

For small quark masses, we can substitute the ap-

proximation $\varphi(x) \rightarrow (x\bar{x})^\beta$ for the $n = 0$ ground state, and carry the integration in (B4) with the result

$$d_V^0(z) = C \frac{\bar{z}}{z} \Gamma[2\beta] \Gamma[1+2\beta] {}_2\tilde{F}_1[1, 1+2\beta, 1+4\beta, z] \quad (\text{B6})$$

where \tilde{F} is the regularized confluent hypergeometric function, and with the normalization fixed through

$$4C\beta\Gamma[2\beta]\Gamma[1+2\beta] \frac{(1+1/(1-4\beta) + \psi(2\beta) - \psi(4\beta-1))}{(-1+2\beta)\Gamma[1+4\beta]} = 1, \quad (\text{B7})$$

where $\psi(z)$ is the digamma function. Eq. (B4) indicates that the differential cross section for the inclusive process is also characterized by d_V^n FFs, as Feynman suggested in the parton model proposal. However, these FFs follow solely from the planar decays of mesons in the large N_c limit, and not from crossing the leading order handbag diagram as per weak coupling and factorization in the light front analysis, hence the difference between $d_V^n(z)$ and $d_{DLY}(z)$ which follows from the crossing argument.

Remarkably, (B4)-(B7) exhibit scaling with the end point behavior $d_V^n(z \sim 1) \sim \bar{z}^{2\beta}$ and $d_V^n(z \sim 0) \sim 1/z$, as per the QCD2 DLY result (B1), and also in agreement with QED2. However, the overall coefficients multiplying the scaling laws are different. In Fig. 8 we show the light quark fragmentation functions in QCD2 following from (B4)-(B5), for $\beta = 0$ (solid blue line) and $\beta = 0.2$ (solid red line), which is to be compared to Fig. 3 for QED2. The behaviors are comparable but not identical.

Additional planar contributions from splittings of the fragmented mesons to additional mesons con-

tribute to the same order. They correspond to a hadronic out-in cascade of mesons in the large number of colors limit [69].

For the meson pair decay, the total inclusive cross section in QCD2 in the 't Hooft limit yields the expected R-ratio scaling, when the sum over all intermediate meson resonances with width $1/N_c$ is carried out for fixed \sqrt{s} [69],

$$\sigma_{e^+e^-} = \sum_{n,f} e_f^2 \sigma_n \rightarrow R = \sum_f N_c e_f^2 \quad (\text{B8})$$

The R-ratio is dominated by the short distance UV physics. The same observation was made for the F2 structure function [69]. The scaling laws in QCD2 are recovered from free field theory, when the 't Hooft limit is carried carefully. In QCD4 they follow from asymptotic freedom at weak coupling.

Appendix C: Convergence of $C(Z)$ with time

In order to get an understanding of how much the qFF at a fixed lattice site varies with asymptotic

time, we show the time evolution of the four inner most points ($Z = 0, 1, 2, 3$). From Fig. 9 it is clear

that the maximum at $Z = 0$ rapidly converges to a constant with small oscillations.

-
- [1] John C. Collins, Davison E. Soper, and George F. Sterman, “Factorization of Hard Processes in QCD,” *Adv. Ser. Direct. High Energy Phys.* **5**, 1–91 (1989), [arXiv:hep-ph/0409313](#).
- [2] John Collins, *Foundations of Perturbative QCD*, Cambridge Monographs on Particle Physics, Nuclear Physics and Cosmology, Vol. 32 (Cambridge University Press, 2023).
- [3] Curtis G. Callan, Jr. and David J. Gross, “High-energy electroproduction and the constitution of the electric current,” *Phys. Rev. Lett.* **22**, 156–159 (1969).
- [4] David J. Gross and Frank Wilczek, “Ultraviolet Behavior of Nonabelian Gauge Theories,” *Phys. Rev. Lett.* **30**, 1343–1346 (1973).
- [5] H. David Politzer, “Reliable Perturbative Results for Strong Interactions?” *Phys. Rev. Lett.* **30**, 1346–1349 (1973).
- [6] Xiangdong Ji, “Parton Physics on a Euclidean Lattice,” *Phys. Rev. Lett.* **110**, 262002 (2013), [arXiv:1305.1539 \[hep-ph\]](#).
- [7] Anatoly V. Radyushkin, “Pion Distribution Amplitude and Quasi-Distributions,” *Phys. Rev. D* **95**, 056020 (2017), [arXiv:1701.02688 \[hep-ph\]](#).
- [8] Yan-Qing Ma and Jian-Wei Qiu, “Extracting Parton Distribution Functions from Lattice QCD Calculations,” *Phys. Rev. D* **98**, 074021 (2018), [arXiv:1404.6860 \[hep-ph\]](#).
- [9] Jian-Hui Zhang, Jiunn-Wei Chen, Xiangdong Ji, Luchang Jin, and Huey-Wen Lin, “Pion Distribution Amplitude from Lattice QCD,” *Phys. Rev. D* **95**, 094514 (2017), [arXiv:1702.00008 \[hep-lat\]](#).
- [10] Xiangdong Ji, Andreas Schäfer, Xiaonu Xiong, and Jian-Hui Zhang, “One-Loop Matching for Generalized Parton Distributions,” *Phys. Rev. D* **92**, 014039 (2015), [arXiv:1506.00248 \[hep-ph\]](#).
- [11] Gunnar S. Bali, Vladimir M. Braun, Benjamin Gläsel, Meinulf Göckeler, Michael Gruber, Fabian Hutzler, Piotr Korcyl, Andreas Schäfer, Philipp Wein, and Jian-Hui Zhang, “Pion distribution amplitude from Euclidean correlation functions: Exploring universality and higher-twist effects,” *Phys. Rev. D* **98**, 094507 (2018), [arXiv:1807.06671 \[hep-lat\]](#).
- [12] Constantia Alexandrou, Krzysztof Cichy, Martha Constantinou, Karl Jansen, Aurora Scapellato, and Fernanda Steffens, “Transversity parton distribution functions from lattice QCD,” *Phys. Rev. D* **98**, 091503 (2018), [arXiv:1807.00232 \[hep-lat\]](#).
- [13] Taku Izubuchi, Luchang Jin, Christos Kallidonis, Nikhil Karthik, Swagato Mukherjee, Peter Petreczky, Charles Shugert, and Sergey Syritsyn, “Valence parton distribution function of pion from fine lattice,” *Phys. Rev. D* **100**, 034516 (2019), [arXiv:1905.06349 \[hep-lat\]](#).
- [14] Taku Izubuchi, Xiangdong Ji, Luchang Jin, Iain W. Stewart, and Yong Zhao, “Factorization Theorem Relating Euclidean and Light-Cone Parton Distributions,” *Phys. Rev. D* **98**, 056004 (2018), [arXiv:1801.03917 \[hep-ph\]](#).
- [15] Sebastian Griener, Kazuki Ikeda, and Ismail Zahed, “Quasiparton distributions in massive QED2: Toward quantum computation,” *Phys. Rev. D* **110**, 076008 (2024), [arXiv:2404.05112 \[hep-ph\]](#).
- [16] R. D. Field and R. P. Feynman, “A Parametrization of the Properties of Quark Jets,” *Nucl. Phys. B* **136**, 1 (1978).
- [17] Bo Andersson, *The Lund Model*, Cambridge Monographs on Particle Physics, Nuclear Physics and Cosmology, Vol. 7 (Cambridge University Press, 2023).
- [18] Raktim Abir *et al.*, “The case for an EIC Theory Alliance: Theoretical Challenges of the EIC,” (2023), [arXiv:2305.14572 \[hep-ph\]](#).
- [19] R. Abdul Khalek *et al.*, “Science Requirements and Detector Concepts for the Electron-Ion Collider: EIC Yellow Report,” *Nucl. Phys. A* **1026**, 122447 (2022), [arXiv:2103.05419 \[physics.ins-det\]](#).
- [20] John C. Collins and Davison E. Soper, “Parton Distribution and Decay Functions,” *Nucl. Phys. B* **194**, 445–492 (1982).
- [21] Andreas Metz and Anselm Vossen, “Parton Fragmentation Functions,” *Prog. Part. Nucl. Phys.* **91**, 136–202 (2016), [arXiv:1607.02521 \[hep-ex\]](#).
- [22] T. Ito, W. Bentz, I. C. Cloet, A. W. Thomas, and K. Yazaki, “The NJL-jet model for quark fragmentation functions,” *Phys. Rev. D* **80**, 074008 (2009), [arXiv:0906.5362 \[nucl-th\]](#).

- [23] Seung-il Nam and Chung-Wen Kao, “Fragmentation functions and parton distribution functions for the pion with the nonlocal interactions,” *Phys. Rev. D* **85**, 034023 (2012), [arXiv:1111.4444 \[hep-ph\]](#).
- [24] Hrayr H. Matevosyan, Wolfgang Bentz, Ian C. Cloet, and Anthony W. Thomas, “Transverse Momentum Dependent Fragmentation and Quark Distribution Functions from the NJL-jet Model,” *Phys. Rev. D* **85**, 014021 (2012), [arXiv:1111.1740 \[hep-ph\]](#).
- [25] S. D. Drell, Donald J. Levy, and Tung-Mow Yan, “A Theory of Deep Inelastic Lepton-Nucleon Scattering and Lepton Pair Annihilation Processes. 1.” *Phys. Rev.* **187**, 2159–2171 (1969).
- [26] S. D. Drell, Donald J. Levy, and Tung-Mow Yan, “A Theory of Deep Inelastic Lepton Nucleon Scattering and Lepton Pair Annihilation Processes. 2. Deep Inelastic electron Scattering,” *Phys. Rev. D* **1**, 1035–1068 (1970).
- [27] John B. Kogut and Leonard Susskind, “Hamiltonian Formulation of Wilson’s Lattice Gauge Theories,” *Phys. Rev. D* **11**, 395–408 (1975).
- [28] Pascual Jordan and Eugene P. Wigner, “About the Pauli exclusion principle,” *Z. Phys.* **47**, 631–651 (1928).
- [29] Henry Lamm, Scott Lawrence, and Yukari Yamauchi (NuQS), “Parton physics on a quantum computer,” *Phys. Rev. Res.* **2**, 013272 (2020), [arXiv:1908.10439 \[hep-lat\]](#).
- [30] M. G. Echevarria, I. L. Egusquiza, E. Rico, and G. Schnell, “Quantum simulation of light-front parton correlators,” *Phys. Rev. D* **104**, 014512 (2021), [arXiv:2011.01275 \[quant-ph\]](#).
- [31] Michael Kreshchuk, Shaoyang Jia, William M. Kirby, Gary Goldstein, James P. Vary, and Peter J. Love, “Simulating Hadronic Physics on NISQ devices using Basis Light-Front Quantization,” *Phys. Rev. A* **103**, 062601 (2021), [arXiv:2011.13443 \[quant-ph\]](#).
- [32] Adrián Pérez-Salinas, Juan Cruz-Martinez, Abdulla A. Alhajri, and Stefano Carrazza, “Determining the proton content with a quantum computer,” *Phys. Rev. D* **103**, 034027 (2021), [arXiv:2011.13934 \[hep-ph\]](#).
- [33] Tianyin Li, Xingyu Guo, Wai Kin Lai, Xiaohui Liu, Enke Wang, Hongxi Xing, Dan-Bo Zhang, and Shi-Liang Zhu (QuNu), “Partonic collinear structure by quantum computing,” *Phys. Rev. D* **105**, L111502 (2022), [arXiv:2106.03865 \[hep-ph\]](#).
- [34] Wenyang Qian, Robert Basili, Soham Pal, Glenn Luecke, and James P. Vary, “Solving hadron structures using the basis light-front quantization approach on quantum computers,” *Phys. Rev. Res.* **4**, 043193 (2022), [arXiv:2112.01927 \[quant-ph\]](#).
- [35] Tianyin Li, Xingyu Guo, Wai Kin Lai, Xiaohui Liu, Enke Wang, Hongxi Xing, Dan-Bo Zhang, and Shi-Liang Zhu (QuNu), “Exploring light-cone distribution amplitudes from quantum computing,” *Sci. China Phys. Mech. Astron.* **66**, 281011 (2023), [arXiv:2207.13258 \[hep-ph\]](#).
- [36] Torsten V. Zache, Daniel González-Cuadra, and Peter Zoller, “Fermion-qudit quantum processors for simulating lattice gauge theories with matter,” *Quantum* **7**, 1140 (2023), [arXiv:2303.08683 \[quant-ph\]](#).
- [37] Julian S. Schwinger, “Gauge Invariance and Mass. 2.” *Phys. Rev.* **128**, 2425–2429 (1962).
- [38] N. Klco, E. F. Dumitrescu, A. J. McCaskey, T. D. Morris, R. C. Pooser, M. Sanz, E. Solano, P. Lougovski, and M. J. Savage, “Quantum-classical computation of Schwinger model dynamics using quantum computers,” *Phys. Rev. A* **98**, 032331 (2018), [arXiv:1803.03326 \[quant-ph\]](#).
- [39] Roland C. Farrell, Marc Illa, Anthony N. Ciavarella, and Martin J. Savage, “Scalable Circuits for Preparing Ground States on Digital Quantum Computers: The Schwinger Model Vacuum on 100 Qubits,” *PRX Quantum* **5**, 020315 (2024), [arXiv:2308.04481 \[quant-ph\]](#).
- [40] Roland C. Farrell, Marc Illa, Anthony N. Ciavarella, and Martin J. Savage, “Quantum Simulations of Hadron Dynamics in the Schwinger Model using 112 Qubits,” (2024), [arXiv:2401.08044 \[quant-ph\]](#).
- [41] T. V. Zache, N. Mueller, J. T. Schneider, F. Jendrzewski, J. Berges, and P. Hauke, “Dynamical Topological Transitions in the Massive Schwinger Model with a θ Term,” *Phys. Rev. Lett.* **122**, 050403 (2019), [arXiv:1808.07885 \[quant-ph\]](#).
- [42] Marco Rigobello, Simone Notarnicola, Giuseppe Magnifico, and Simone Montangero, “Entanglement generation in (1+1)D QED scattering processes,” *Phys. Rev. D* **104**, 114501 (2021), [arXiv:2105.03445 \[hep-lat\]](#).
- [43] Dmitri E. Kharzeev and Yuta Kikuchi, “Real-time chiral dynamics from a digital quantum simulation,” *Phys. Rev. Res.* **2**, 023342 (2020), [arXiv:2001.00698 \[hep-ph\]](#).
- [44] Adrien Florio, David Frenklakh, Kazuki Ikeda, Dmitri Kharzeev, Vladimir Korepin, Shuzhe Shi, and Kwangmin Yu, “Real-Time Nonperturbative Dynamics of Jet Production in Schwinger Model: Quantum Entanglement and Vacuum Modification,” *Phys. Rev. Lett.* **131**, 021902 (2023),

- arXiv:2301.11991 [hep-ph].
- [45] Joshua Lin, Di Luo, Xiaojun Yao, and Phiala E. Shanahan, “Real-time Dynamics of the Schwinger Model as an Open Quantum System with Neural Density Operators,” (2024), arXiv:2402.06607 [hep-ph].
- [46] Kyle Lee, James Mulligan, Felix Ringer, and Xiaojun Yao, “Liouvillian dynamics of the open Schwinger model: String breaking and kinetic dissipation in a thermal medium,” *Phys. Rev. D* **108**, 094518 (2023), arXiv:2308.03878 [quant-ph].
- [47] Wibe A. de Jong, Kyle Lee, James Mulligan, Mateusz Płoskoń, Felix Ringer, and Xiaojun Yao, “Quantum simulation of nonequilibrium dynamics and thermalization in the Schwinger model,” *Phys. Rev. D* **106**, 054508 (2022), arXiv:2106.08394 [quant-ph].
- [48] Ron Belyansky, Seth Whitsitt, Niklas Mueller, Ali Fahimniya, Elizabeth R. Bennewitz, Zohreh Davoudi, and Alexey V. Gorshkov, “High-Energy Collision of Quarks and Mesons in the Schwinger Model: From Tensor Networks to Circuit QED,” *Phys. Rev. Lett.* **132**, 091903 (2024), arXiv:2307.02522 [quant-ph].
- [49] João Barata, Wenjie Gong, and Raju Venugopalan, “Realtime dynamics of hyperon spin correlations from string fragmentation in a deformed four-flavor Schwinger model,” (2023), arXiv:2308.13596 [hep-ph].
- [50] Adrien Florio, “Two-fermion negativity and confinement in the Schwinger model,” *Phys. Rev. D* **109**, L071501 (2024), arXiv:2312.05298 [hep-th].
- [51] Jürgen Berges, Stefan Floerchinger, and Raju Venugopalan, “Thermal excitation spectrum from entanglement in an expanding quantum string,” *Phys. Lett. B* **778**, 442–446 (2018), arXiv:1707.05338 [hep-ph].
- [52] Jürgen Berges, Stefan Floerchinger, and Raju Venugopalan, “Dynamics of entanglement in expanding quantum fields,” *JHEP* **04**, 145 (2018), arXiv:1712.09362 [hep-th].
- [53] Adrien Florio and Dmitri E. Kharzeev, “Gibbs entropy from entanglement in electric quenches,” *Phys. Rev. D* **104**, 056021 (2021), arXiv:2106.00838 [hep-th].
- [54] Sebastian Griener, Dmitri E. Kharzeev, and Ismail Zahed, “Entanglement in a holographic Schwinger pair with confinement,” *Phys. Rev. D* **108**, 086030 (2023), arXiv:2305.07121 [hep-th].
- [55] Sebastian Griener, Dmitri E. Kharzeev, and Ismail Zahed, “Entanglement entropy in a time-dependent holographic Schwinger pair creation,” *Phys. Rev. D* **108**, 126014 (2023), arXiv:2310.12042 [hep-th].
- [56] Sidney R. Coleman, “More About the Massive Schwinger Model,” *Annals Phys.* **101**, 239 (1976).
- [57] Sebastian Griener, Kazuki Ikeda, Dmitri E. Kharzeev, and Ismail Zahed, “Entanglement in massive Schwinger model at finite temperature and density,” *Phys. Rev. D* **109**, 016023 (2024), arXiv:2312.03172 [hep-th].
- [58] Ivo Sachs and Andreas Wipf, “Finite temperature Schwinger model,” *Helv. Phys. Acta* **65**, 652–678 (1992), arXiv:1005.1822 [hep-th].
- [59] James V. Steele, J. J. M. Verbaarschot, and I. Zahed, “The Invariant fermion correlator in the Schwinger model on the torus,” *Phys. Rev. D* **51**, 5915–5923 (1995), arXiv:hep-th/9407125.
- [60] A. Casher, John B. Kogut, and Leonard Susskind, “Vacuum polarization and the absence of free quarks,” *Phys. Rev. D* **10**, 732–745 (1974).
- [61] William A. Bardeen, I. Bars, Andrew J. Hanson, and R. D. Peccei, “A Study of the Longitudinal Kink Modes of the String,” *Phys. Rev. D* **13**, 2364–2382 (1976).
- [62] I. Bars, “A Quantum String Theory of Hadrons and Its Relation to Quantum Chromodynamics in Two-Dimensions,” *Nucl. Phys. B* **111**, 413–440 (1976).
- [63] Edward Shuryak and Ismail Zahed, “Hadronic structure on the light front. II. QCD strings, Wilson lines, and potentials,” *Phys. Rev. D* **107**, 034024 (2023), arXiv:2111.01775 [hep-ph].
- [64] Tom Banks, S. Raby, Leonard Susskind, John B. Kogut, D. R. T. Jones, P. N. Scharbach, and D. K. Sinclair (Cornell-Oxford-Tel Aviv-Yeshiva), “Strong Coupling Calculations of the Hadron Spectrum of Quantum Chromodynamics,” *Phys. Rev. D* **15**, 1111 (1977).
- [65] Ross Dempsey, Igor R. Klebanov, Silviu S. Pufu, and Bernardo Zan, “Discrete chiral symmetry and mass shift in the lattice Hamiltonian approach to the Schwinger model,” *Phys. Rev. Res.* **4**, 043133 (2022), arXiv:2206.05308 [hep-th].
- [66] Hugh Bergknoff, “Physical Particles of the Massive Schwinger Model,” *Nucl. Phys. B* **122**, 215–236 (1977).
- [67] Gerard 't Hooft, “A Two-Dimensional Model for Mesons,” *Nucl. Phys. B* **75**, 461–470 (1974).
- [68] Yi-zhang Mo and Robert J. Perry, “Basis function calculations for the massive Schwinger model in the light front Tamm-Dancoff approximation,” *J. Com-*

- put. Phys. **108**, 159–174 (1993).
- [69] Martin B. Einhorn, “Failure of the Parton Model in Inclusive electron-Positron Annihilation,” *Phys. Rev. D* **15**, 3037 (1977).
- [70] Yu Jia, Zhewen Mo, and Xiaonu Xiong, “Heavy quark fragmentation function in two-dimensional QCD in $N_c \rightarrow \infty$ limit,” *Eur. Phys. J. C* **83**, 1169 (2023), arXiv:2310.17640 [hep-ph].